Visualization of In Situ Intracellular Aggregation of Two Cataract–Associated Human γ-Crystallin Mutants: Lose a Tail, Lose Transparency

Venu Talla,[1] *Narayanaswamy Srinivasan,*[2] *and Dorairajan Balasubramanian*[1]

Purpose. To understand the molecular features underlying autosomal dominant congenital cataracts caused by the deletion mutations W156X in human γD-crystallin and W157X in human γC-crystallin.

Methods. Normal and mutant cDNAs (with the enhanced green fluorescent protein [EGFP] tag in the front) were cloned into the pEGFP-C1 vector, transfected into various cell lines, and observed under a confocal microscope for EGFP fluorescence. Normal and W156X γD cDNAs were also cloned into the pET21a(+) vector, and the recombinant proteins were overexpressed in the BL-21(DE3)pLysS strain of *Escherichia coli*, purified, and isolated. The conformational features, structural stability, and solubility in aqueous solution of the mutant protein were compared with those of the wild type using spectroscopic methods. Comparative molecular modeling was performed to provide additional structural information.

Results. Transfection of the EGFP-tagged mutant cDNAs into several cell lines led to the visualization of aggregates, whereas that of wild-type cDNAs did not. Turning to the properties of the expressed proteins, the mutant molecules show remarkable reduction in solubility. They also seem to have a greater degree of surface hydrophobicity than the wild-type molecules, most likely accounting for self-aggregation. Molecular modeling studies support these features.

Conclusions. The deletion of C-terminal 18 residues of human γC- and γD-crystallins exposes the side chains of several hydrophobic residues in the sequence to the solvent, causing the molecule to self-aggregate. This feature appears to be reflected in situ on the introduction of the mutants in human lens epithelial cells. (*Invest Ophthalmol Vis Sci.* 2008;49:3483–3490) DOI:10.1167/iovs.07-1114

Mutations in the crystallin family of proteins associated with cataract have been identified in human populations across the world.[1–5] Although mutations in all the three families, namely α-, β-, and γ-crystallins, are known to cause cataract, we focus here on two mutations in the human γC- and γD-crystallins. Many of these are single-point mutations (e.g., T5P and R168W in γC-crystallin; R14C, P23T, R36S, Q54A, and R58H in γD-crystallin). Several of these mutated proteins have been cloned, expressed, and isolated, and their properties have been compared with those of the normal (wild-type) γC- and γD-crystallins.[6–13] Such studies have shown that several of these mutations lead to protein self-aggregation and increased light scattering, suggesting a possible relation to lens opacification in vivo. Santhiya et al.[5] have reported a pedigree with autosomal dominant central nuclear cataract, wherein the γD-crystallin was found to have the G470→A mutation in the gene, leading to a premature stop codon, W156X, or Trp156Stop in the protein, which causes the C-terminal residues 156–174 to be deleted. Interestingly, a homologous mutation at the same site, W157X, has been identified recently in China in γC-crystallin in association with patients with congenital cataract (Zhang L, et al. *IOVS* 2007;48:ARVO E-Abstract 2443).

It is these two mutants, W156X human γD- and W157X γC-crystallins, on which we focus attention in this report. We have cloned and expressed the mutant γD-crystallin and compared its solution state properties with those of the wild-type protein. In addition, we have performed comparative molecular modeling for the two mutants and wild-type proteins. Such an analysis of the consequences of the loss of the C-terminal fragment provides insight into the intramolecular and intermolecular interactions that occur in the mutant molecule. Experimental results support the in silico analysis and show that this deletion leads to changes in the properties of the protein, notably reduced solubility and a tendency for self-aggregation. We have indeed been able to visualize such self-aggregation leading to scattering particles in situ, when cDNAs of the mutants are transfected into a variety of cell lines, among them African green monkey kidney (COS1) cells, rat retinal ganglion cells (RGC-5), and notably human lens epithelial (HLE3B) cells. Similar transfections of the cDNA of the wild-type γC- and γD-crystallins did not show any scattering particles. We suggest that these altered properties of the mutants play a role in nuclear cataractogenesis.

Methods

Generation of the pEGFP-Crystallin Constructs

Human cadaveric eye lens (donor age, 56 years) was collected from the Ramayamma International Eye Bank, L.V. Prasad Eye Institute, Hyderabad, India, and total RNA was isolated using reagent (Trizol; Invitrogen, Carlsbad, CA). The first strand was synthesized by RT-PCR using an oligo-dT primer and μ-MLV reverse transcriptase. Human γC- and γD-crystallin cDNAs were amplified from the first strand using gene-specific primers. Primer sequences used to amplify the wild-type γC cDNA were 5′-GC*CTCGA*GGGAAGATCACCTTCTA TG-3′ forward and 5′-GC*GGATCC*TTAATACAAATCCACCACTCT-3′ reverse. Primer sequences used to amplify wild-type γD cDNA were 5′-GC*CTCGA*GG GAAGATCACCCTCTA-3′ forward and 5′-GC*GGATCC*TCAGGAGAAA-TCTATGACTCT-3′ reverse. To amplify the mutant cDNAs, the reverse primer was designed from the site of mutation, which contains the

From the [1]Brien Holden Research Center, Hyderabad Eye Research Foundation, L. V. Prasad Eye Institute, Hyderabad, India; and the [2]Molecular Biophysics Unit, Indian Institute of Science, Bangalore, India.

Supported by the Department of Biotechnology, India; the Council of Scientific and Industrial Research, India; and Wellcome Trust, UK.

Submitted for publication August 25, 2007; revised January 14 and March 15, 2008; accepted June 13, 2008.

Disclosure: **V. Talla**, None; **N. Srinivasan**, None; **D. Balasubramanian**, None

The publication costs of this article were defrayed in part by page charge payment. This article must therefore be marked "*advertisement*" in accordance with 18 U.S.C. §1734 solely to indicate this fact.

Corresponding author: Dorairajan Balasubramanian, Brien Holden Research Center, Hyderabad Eye Research Foundation, L. V. Prasad Eye Institute, Kallam Anji Reddy Campus, Banjara Hills, Hyderabad 500034, India; dbala@lvpei.org.

desired base change. The reverse primer sequence used for the W156X γD cDNA was 5′-GC*GGATCC*CTAGTCCTGGTAGCGCCT-3′, whereas that used for W157X γC cDNA was 5′-GC*GGATCC*CTAGTCCTGGCA CCGCCTGTA-3′. The amplified wild-type and mutant γ-crystallin cDNAs were cloned into predigested pJET vector (blunt end cloning). The recombinant clones were confirmed by PCR and restriction digestion, and the sequences of the cDNAs were confirmed by direct sequencing using an automated sequencer (ABI Prism 320). Mutant and wild-type cDNAs were released from the pJET vector by restriction digestion using *Xho*I and *Bam*HI. The released cDNAs were subcloned into the *Xho*I and *Bam*HI sites of the pEGFP-C1 vector, which resulted in the enhanced green fluorescent protein (EGFP)-γ-crystallin proteins. pEGFP-C1 encodes a red-shifted variant of wild-type GFP, which has been optimized for brighter fluorescence and higher expression in mammalian cells (excitation maximum, 488 nm; emission maximum, 507 nm).[14–16]

Cell Culture and Transfections

The HLE 3B, COS1, and RGC-5 cell lines were cultured in Dulbecco modified Eagle medium (DMEM) supplemented with 10% fetal calf serum (FCS) in a 5% humidified CO_2 incubator at 37°C. One day before transfection, the cells (60,000) were seeded on a 22-mm coverslip in a six-well culture plate and incubated at 37°C in a 5% humidified CO_2 incubator. The medium was removed after 24 hours and replaced with serum-free DMEM and transfected with the vectors using reagent (Lipofectamine 2000; Invitrogen) at a 1:2 ratio (~500 ng vector/1 μL reagent). After incubation for 4 to 5 hours, the serum-free medium was replaced with complete medium (DMEM + 10% FCS), and incubation continued up to 24 hours for imaging analysis. The constructs used for the transfections were pEGFP-WTγC, pEGFP-WTγD, pEGFP-W157X γC, pEGFP-W156X γD, and pEGFP-C1.

Confocal Microscopic Imaging

After incubation, the transfected cells were washed with PBS and fixed using absolute ice-cold methanol for 10 to 15 minutes. The cells were washed with PBS three times for 5 minutes each and were stained with propidium iodide for 1 minute. An excess amount of the stain was removed by a PBS wash. Coverslips with the cells were then mounted using 50% glycerol in PBS and observed using a laser scanning confocal microscope (LSM510; Carl Zeiss, Jena, Germany). The excitation lasers used were 488/543 nm; the emission of green fluorescence was collected using the 505- to 530-nm band-pass filter (channel 2), and that of red fluorescence was collected using the 585- to 615-nm band-pass filter (channel 3).

Immunofluorescence for γ-Crystallins

The cDNAs of wild-type and mutant human γD-crystallin were cloned into pcDNA3.1(−) vector under the *Xho*I and *Bam*HI sites and were transfected into RGC5 and HLE3 cell lines on 22-mm^2 coverslips. Cells were fixed using 4% formaldehyde and permeabilized using PBS containing 0.1% Triton X-100 for 10 minutes. Cells were then washed three times with PBS and incubated with anti-human γ-crystallin antibody (raised in rabbit; a kind gift of J. Samuel Zigler, Jr, The Wilmer Eye Institute, Johns Hopkins University, Baltimore, MD) for 1 hour. They were then washed three times and incubated with tetramethylrhodamine isothiocyanate (TRITC)-conjugated anti–rabbit antibody. Excess and unbound antibody was removed by washing the coverslips with PBS, mounted on glass slides, and observed using a confocal microscope. Excitation lasers used were 514/543 nm, and fluorescence emission was collected using 585 to 615 nm band-pass filter.

Western Blotting

Cells were harvested from T-25 culture flasks 48 hours after transfection and were suspended in 300 μL Brij buffer (0.1 M Tris Cl, pH 7.5, 0.5 M NaCl, 1% Brij 96, 1% NP40, 2 mM EDTA, 1 mM phenylmethylsulfonyl fluoride [PMSF], 3 μg/mL aprotinin) and lysed by sonication 4 × 30 seconds (30-second intervals) at 35% amplitude using a high-intensity ultrasonic processor (Sonics Vibra Cell; Sonics & Materials Inc., Newtown, CT). The cell lysate was centrifuged at 13,000 rpm, 4°C, for 15 minutes. Supernatant was separated, and the pellet was dissolved in 50 μL of 1× SDS loading buffer. The lysate and the cell pellet dissolved in SDS loading buffer were separated on 12% SDS-PAGE and blotted onto nitrocellulose membrane using a horizontal semidry blotting apparatus (Amersham Biosciences). Nonspecific binding sites were blocked with TBS (0.05% Tween 20 and 5% nonfat milk in PBS) overnight at 4°C. The membrane was incubated with rabbit monoclonal antibody raised against purified EGFP (Santa Cruz Biotechnology, Santa Cruz, CA), 1:1000, in blocking buffer for 2 hours at room temperature. Three TBST (0.05% Tween 20 in PBS) washes (5 minutes each) were given to remove the unbound antibody, and the membrane was incubated with horseradish peroxidase (HRP)–conjugated anti–rabbit immunoglobulin G (1:6000 in blocking buffer; Sigma Aldrich, St. Louis, MO) for 1 hour at room temperature. An excessive amount of the secondary antibody was removed by washing the membrane three times (5 minutes each) with TBST, and the bands were visualized with the enhanced chemiluminescence method. Briefly, the membrane was incubated for 1 minute with HRP substrate (1:1 ratio of solution I [100 mM Tris, pH 8.5, 0.4 mM coumaric acid, 2.5 mM luminol] and solution II [100 mM Tris Cl, pH 8.5, 5 mM H_2O_2]). The substrate was drained, and the membrane was wrapped in plastic wrap and exposed to hyperfilm x-ray sheet for the desired length of time (1 minute, 2 minutes, 5 minutes, 10 minutes). The hyperfilm exposed to membrane was then developed and fixed using an x-ray developer and fixative.

Cloning of Wild-Type and W156X Mutant γD-Crystallins

Human γD-crystallin cDNA was amplified from the first strand using gene-specific primers. The primers used were the same as those shown except for a change in restriction enzyme site. The *Nde*I restriction site was introduced in the forward primers, and the *Hin*dIII site was introduced in all reverse primers. The amplified wild-type and mutant γD-crystallin cDNAs were cloned into the *Sma*I site of the pBSSK vector. Both constructs were sequenced using T3 and T7 primers to ensure that no additional mutations were present. The inserts were released from the vector and further subcloned into the *Nde*I/*Hin*dIII site of the pET21a(+) vector.

Overexpression and Purification of Recombinant Proteins

The protocol followed was essentially the same as that described earlier.[11] Briefly, the recombinant constructs pET21a(+)-wt γD and pET21a(+)-W156X γD were transformed into *BL21(DE3)pLysS* cells. For the overexpression of recombinant proteins, bacterial cultures were grown at 37°C in the presence of ampicillin and chloramphenicol to an absorbance value of 0.6 at 600 nm. Expression of γ-crystallins was induced by the addition of 1 mM isopropyl 1-thio-D-galactopyranoside, and the cultures were grown for an additional 4 to 5 hours. Cells were pelleted down, and the proteins were isolated as mentioned in a previous report.[17] Wild-type γD-crystallin was fractionated exclusively to the soluble fraction, whereas the mutant was largely found in inclusion bodies. Wild-type γD-crystallin was purified by ammonium sulfate fractionation, size exclusion, and DEAE-cellulose ion-exchange chromatography.

For the isolation of mutant γD-crystallin from inclusion bodies, the cells were harvested from 1-L culture by centrifugation at 5000 rpm at 4°C for 5 minutes and were suspended in 40 mL ice-cold buffer containing 20 mM Tris HCl, pH 7.5, containing 20% wt/vol sucrose and 1 mM EDTA. The cells were centrifuged at 11,000 rpm for 5 minutes at 4°C, and the pellet was resuspended in 40 mL ice-cold water. The cell pellet was collected by centrifugation at 11,000 rpm for 5 minutes, resuspended in 10 mL buffer P (10 mM PBS containing 5 mM EDTA, 20 μg/mL aprotinin, and 1 mM PMSF) and repeatedly sonicated (12 × 15 seconds, with 30-second intervals). Inclusion bodies were harvested by

centrifugation at 11,000 rpm for 30 minutes, and the pellet was resuspended in 1 mL buffer P and 40 mL another buffer made up of 10 mM PBS, pH 7.2, containing 25% wt/vol sucrose, 5 mM EDTA, 1% Triton X-100, and 1 mM PMSF. The suspension was centrifuged at 20,000 rpm for 10 minutes and was washed twice. The final pellet was resuspended in 5 mL of 50 mM Tris HCl, pH 8.0, containing 5 mM EDTA, 8 M urea, and 5 mM dithiothreitol (DTT), at room temperature and was stored at −20°C or continued with the folding protocol immediately. Solubilized protein was diluted 10-fold using an ice-cold folding buffer (50 mM HEPES, pH 7.5, containing 0.2 M NaCl, 1 mM DTT, 400 mM L-arginine and 1 mM PMSF) under vigorous stirring. The protein mixture was dialyzed against buffer containing 50 mM Tris HCl, pH 8.0, at 4°C with four changes of buffer. The dialyzed protein was further purified by size exclusion chromatography. Wild-type γD-crystallin was also treated similarly to mutant. The purity of the wild-type and mutant γD-crystallin proteins was confirmed by SDS-PAGE analysis. Protein concentrations were calculated using the Bradford method of protein estimation.

Spectroscopic Analysis of Recombinant Proteins

Intrinsic fluorescence spectra were recorded at 20°C using a fluorescence spectrophotometer (F-2500; Hitachi, Yokohama, Japan) equipped with a circulating water bath (model F-12, Julabo; Sigma Aldrich) to control the sample temperature. Fluorescence emission spectra were recorded in the range of 300 to 400 nm using an excitation wavelength of 295 nm, with 2.5 nm excitation and emission slits. Extrinsic fluorescence spectra of proteins were recorded using 100 μM 8-anilinonaphthalene-1-sulfonate (ANS) as an external (surface hydrophobicity) probe. Spectra were recorded in the range of 400 to 600 nm, with an excitation wavelength of 390 nm. The protein concentrations used were 0.1 mg/mL in Tris HCl buffer, pH 7.4. Circular dichroism (CD) spectra were recorded with a spectropolarimeter (J-715; Jasco, Easton, MD) at room temperature. Protein concentrations of 0.25 mg/mL were used for recording far-ultraviolet light CD spectra (250–190 nm) with 0.1-cm path length quartz cells. Three scans of each spectrum were averaged smoothed, and baselines (buffer alone) were subtracted for all the spectra mentioned.

Guanidinium Chloride–Induced Unfolding and Refolding

Unfolding experiments were carried out by diluting the wild-type and mutant γD-crystallins to 25 μg/mL into increasing concentrations of guanidinium (Gdn) HCl from 0 to 6 M. Unfolding samples were incubated at room temperature for 24 h, by which time equilibrium had been reached. Refolding experiments were carried out by initially preparing an unfolded stock solution of 100 μg/mL proteins by incubation for 24 hours in 6M Gdn HCl. Unfolded proteins were refolded by dilution into folding buffer (50 mM HEPES, pH 7.5, containing 0.2 M NaCl, 1 mM DTT, 400 mM L-arginine, and 1 mM PMSF) to a final concentration of 10 μg/mL protein and 1 to 5 M denaturant. Fluorescence emission spectra were recorded in the range of 300 to 400 nm with an excitation wavelength of 295 nm, and baseline spectra of Gdn HCl solutions from 0 to 6 M were subtracted. Data were analyzed by plotting the fluorescence intensity at 360/320 nm compared with the Gdn HCl concentration.

Thermal Stability Measurement

Thermal denaturation of the wild-type and mutant crystallins was studied by monitoring the temperature-dependent changes in the Trp emission intensity and wavelength, measured at 5° intervals between 20° to 70°C. An equilibrium time of 15 minutes was allowed for each temperature, and the temperature was controlled using a (Julabo) circulating water bath. Fluorescence spectra were collected in the range of 300 to 400 nm using excitation wavelength of 295 nm, and the baseline spectra of the buffer alone (Tris HCl, pH 7.2) were subtracted. The data were analyzed by plotting the percentage decrease in fluorescence emission versus temperature. For the time-dependent, light-scattering measurements, the fluorescence spectrophotometer was used with excitation and emission wavelengths set at 600 nm, and measurements were performed at 65°C. Solutions of the wild-type and mutant proteins, each at 10 μg/mL in Tris HCl buffer, were taken, and the scattering at 600 nm was measured as a function of time, up to 1200 seconds.

Molecular Modeling

The three-dimensional structure of the human γC-crystallin was modeled on the basis of the crystal structure of bovine γB-crystallin (ID 1 gcs; Protein Data Bank, ftp://ftp.wwpdb.org).[18] The structure was generated using homology modeling software (MODELER,[19] version 7). The human γD-crystallin model was retrieved from the crystal structure data provided by Basak et al.[8] in the Protein Data Bank (ID 1HK0). The effect of the deletion on the structure of the two proteins was analyzed using the software SETOR. Surface charge distributions of the wild-type and mutant molecules were estimated and visualized using the software GRASP. The three-dimensional solid model representations were generated using the software SETOR.[20] The methods used and their details are provided in our earlier paper.[11]

Results

Mutant Proteins Aggregate In Situ in Cells

Figure 1 (column 1) shows the confocal microscopic images of EGFP (Figs. 1C, 1F, control), EGFP-tagged wild-type γD and γC (Figs. 1A, 1D), and tagged W156X human γD and W157X human γC cDNAs (Figs. 1B, 1E, respectively), transfected in COS1 cell lines. Although EGFP and the wild-type molecules are seen to be uniformly present, with no special features, in the cytoplasm and nuclei of the cells, the mutant molecule is seen to clump up into scattering particles, largely in the cytoplasm. The tendency of EGFP to locate freely in the cytoplasm and nucleus (visualized by red) seems to be reduced when fused with the mutant (but not when fused with the wild type). The mutant γC-crystallin behaves similarly to mutant γD-crystallin in aggregating and forming light-scattering particles. Column 2 of Figure 1 shows the results of similar experiments, this time using the retinal ganglion cell line RGC5 for transfection. Here again, though the wild-type molecules (Figs. 1A, 1D) display normal distribution across the cell, the mutant γD- and γC-crystallins (Figs. 1B, 1E, respectively) are seen to aggregate and form scattering particles. These results are similar to the scattering particles seen when the V76D mutant of murine γD-crystallin is transfected into mouse lens epithelial cells[21]; the T5P mutant of γC-crystallin was transfected into HEK293 cell lines by Pigaga and Quinlan.[22]

Although crystallins are reported to occur in non–lens tissues and cells (such as the retina[23,24]), they are found in higher amounts in the lens. Thus, it is more appropriate to study the behavior of the mutants in lens cells. Column 3 of Figure 1 compares the behavior of wild-type (Figs. 1A, 1D) and mutant γD- and γC-crystallins (Figs. 1B, 1E, respectively) when their cDNAs are transfected into the HLE 3B human lens epithelial cell lines. Distinct cytoplasmic localization and clumping to produce scattering particles are displayed by the mutant crystallins.

Whether fusing EGFP to the crystallins might affect the solubility and aggregation properties of the latter was addressed using two approaches. In the first approach, we performed Western blotting with the use of anti–EGFP antibody. We lysed COS-1 cells that were transfected with the fused protein genes and analyzed the presence of the proteins in the soluble and insoluble fraction of the lysate using the anti–EGFP antibody. Fusion with EGFP keeps the wild-type protein in the soluble fraction, and the EGFP-fused mutants are not seen in

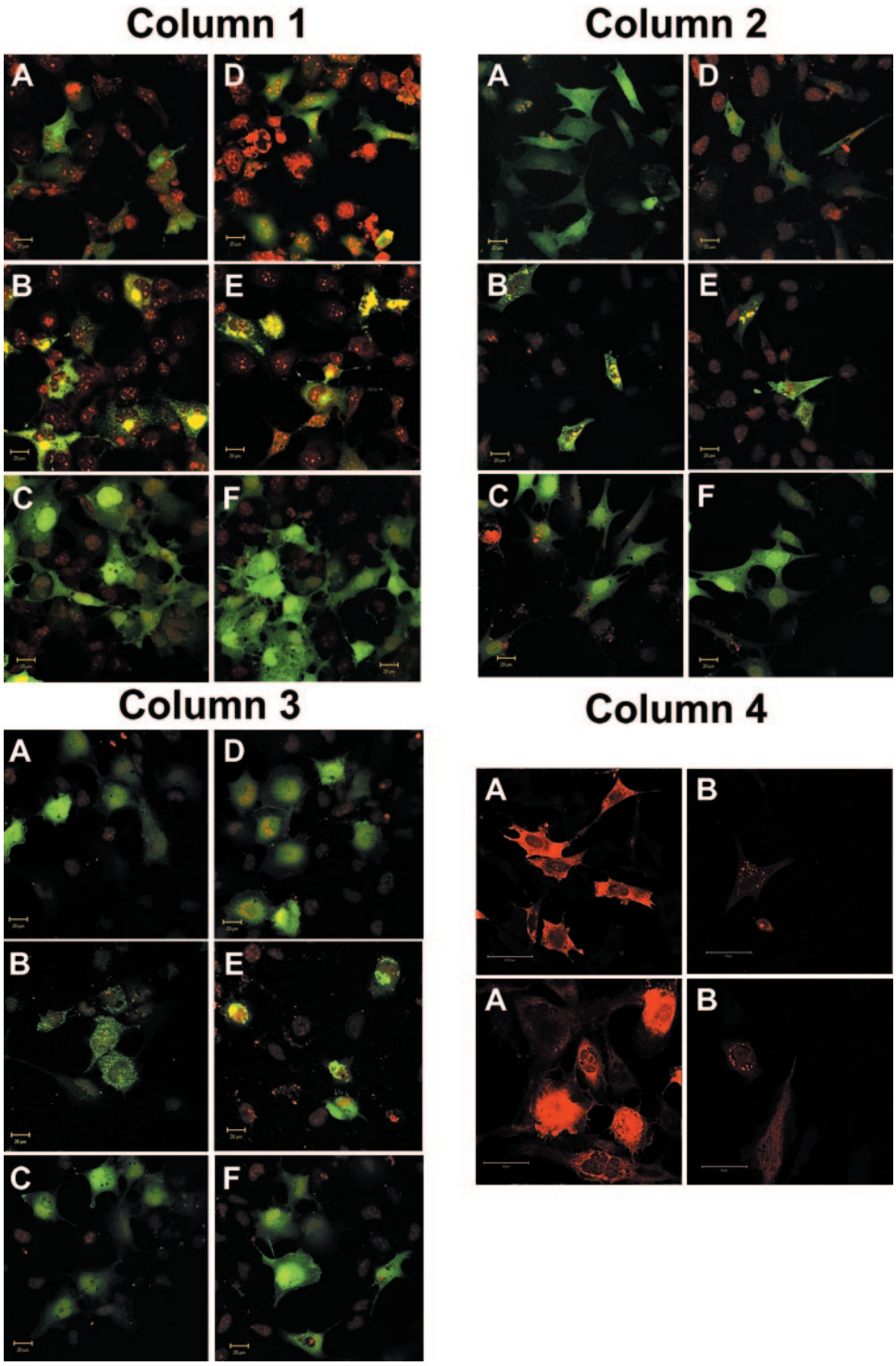

FIGURE 1. Confocal microscopic pictures of cDNAs of EGFP (**C**, **F**), EGFP-tagged wild-type and W156X mutants of human γD-crystallin (**A**, **B**, respectively), and wild-type and W157X mutants of human γC-crystallin (**D**, **E**, respectively), The nuclei of cells were counterstained with propidium iodide and are seen in *red*, whereas the *green* fluorescence is of EGFP. *Column 1*: results of transfection into monkey kidney COS1 cell lines. *Column 2*: results of transfection into rat retinal RGC5 cell lines. *Column 3*: results of transfection into human lens epithelial HLE 3B cell lines. *Column 4*, *top*: images of RGC5 cells transfected with pcDNA3.1(−) recombinant constructs of untagged, neat wild-type (**A**), and W156X human γD-crystallin (**B**), probed with anti-human γ-crystallin antibody (raised in rabbit) and TRITC conjugated anti-rabbit secondary antibody. *Bottom*: same images using HLE3B cell lines. (**A**) Wild type. (**B**) Mutant.

the soluble fraction but only in the insoluble one. In the second approach, we transfected cDNAs of untagged, neat, wild-type, and mutant molecules into RGC5 (and HLE3B) cells and monitored the resultant proteins using anti–human γ-crystallin antibody. Results are displayed in column 4 of Figure 1.

Properties of the Recombinant γD-Crystallins in Solution

To understand the molecular basis behind the formation of such aggregates and scattering particles, we cloned, expressed, isolated, and purified the proteins and compared their properties in the solution state. Figure 2A shows the SDS-PAGE profiles of the wild-type and W156X γD-crystallins. The solubility of the mutant is far lower than that of the wild-type protein. Figure 2B shows the difference in the thermal aggregation profiles of the wild type and the mutant. γ-Crystallins are known to aggregate[25] on heating to 65°C. The light-scattering intensity of the mutant is increased threefold within 15 minutes, whereas that of the wild type is negligible. To probe into the solution state structural differences between the two, we compared their conformational properties.

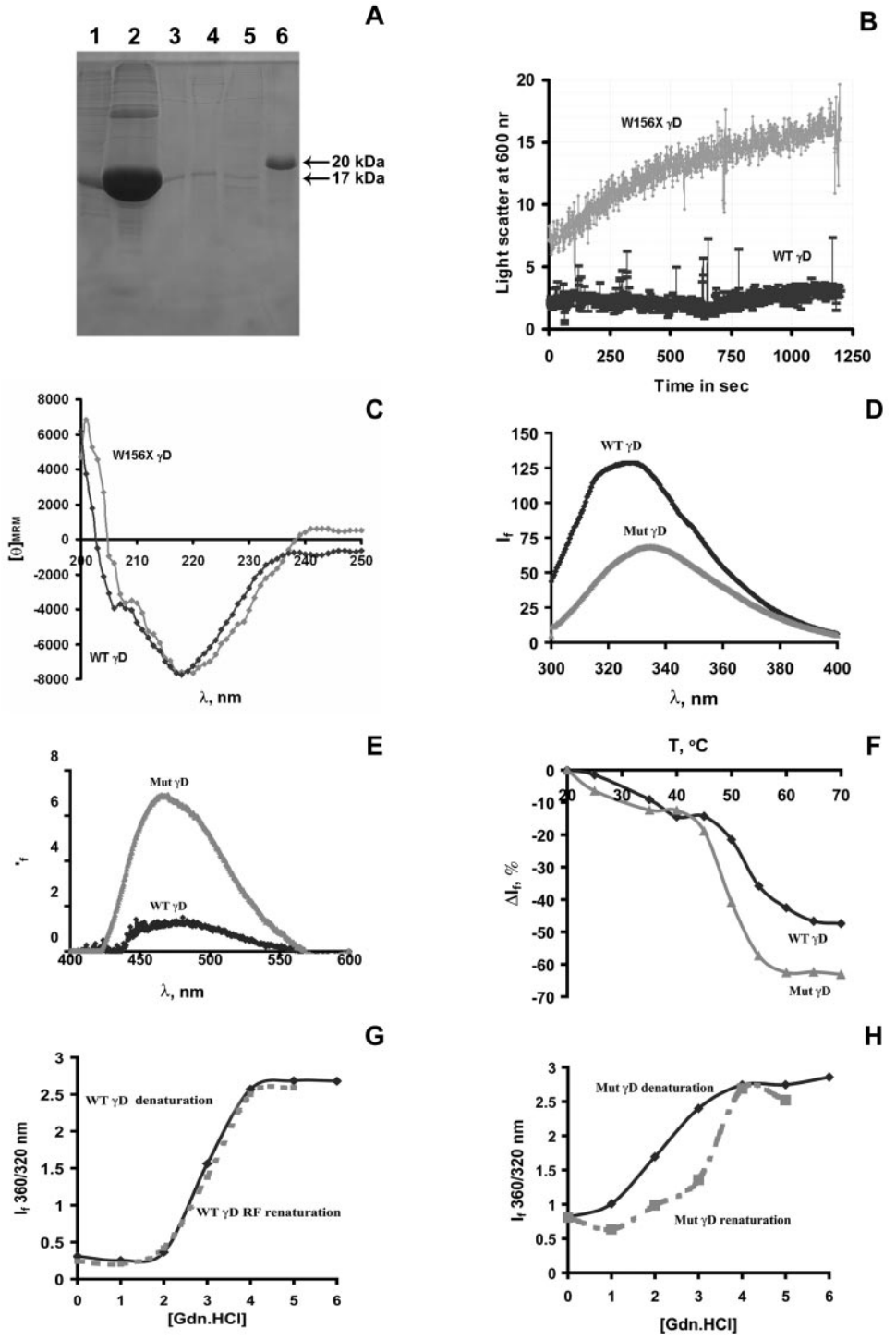

FIGURE 2. (**A**) SDS PAGE ERGs of overexpressed and purified wild-type and mutant human γD-crystallin. *Lane 1*: W156X mutant seen 3 hours after induction. *Lane 2*: mutant seen in inclusion bodies. *Lanes 3–5*: purified and refolded mutant. *Lane 6*: purified wild-type protein. (**B**) Thermal aggregation profiles of wild-type (*bottom*) and W156X (*top*) mutant human γD-crystallin. (**C**) Far-UV CD spectra of the wild-type (WT) and W156X mutant human γD-crystallin. Ellipticity values are expressed in residue molar units. (**D**) Intrinsic fluorescence spectra of wild-type (WT) and mutant samples. λ_{ex}, 295 nm. (**E**) Extrinsic fluorescence of the surface hydrophobicity probe ANS bound to γD-crystallins λ_{ex}, 390 nm. (**F**) Thermal denaturation profiles of the wild-type and W156X mutant. (**G**) Gdn HCl-induced denaturation/renaturation curves of wild-type human γD-crystallin. (**H**) Gdn HCl-induced denaturation/renaturation curves of the W156X mutant. Graphs were constructed by plotting the fluorescence intensity ratio at 360/320 versus Gdn HCl concentration.

Figure 2C compares the circular dichroism spectra of the wild-type and mutant protein, in the (far UV) 250- to 200-nm spectral region, reflecting the secondary structural features of the molecules. Wild-type and mutant proteins display a mean residue molar ellipticity of −8000° at 218 nm, in keeping with earlier reports, suggesting that the proteins are folded in the β-pleated sheet conformation. There are minor differences in the CD spectra between the two proteins, but it is unclear whether this suggests any particularly structurally useful information.

Figure 2D shows the intrinsic fluorescence spectra of wild-type and W156X human γD-crystallins. Although the wild-type molecule shows an emission maximum at 327 nm (in agreement with earlier reports) with an (arbitrary) intensity of approximately 120 U, the mutant emits at 336 nm, with almost half the intensity of the wild-type molecule. The red shift seen in the mutant suggests that the aromatic (predominantly trp) residues are relatively more exposed to the solvent than in the wild-type molecule. Figure 2E shows the extrinsic fluorescence of the surface hydrophobic probe ANS bound to the two proteins. When bound to the wild-type protein, ANS displays its broad emission maximum around 484 nm of relatively low intensity; when bound to the mutant, the probe shows a blue-shifted band around 466 nm with a threefold higher in-

tensity. These data suggest that the mutant molecule has a more pronounced hydrophobic surface.[26]

The structural stability of the mutant is lower than that of the wild-type protein, as seen in the thermal denaturation profiles (Fig. 2F), and chemical denaturation using Gdn HCl as the denaturant too reveals the same. Interestingly, though the refolding curve of the wild-type molecule here traces the same path as the unfolding curve (Fig. 2G), those of the mutant molecule are not superimposed (Fig. 2H); the molecule seems to show hysteresis. Such noncoincidence of the unfolding and refolding pathways is thought to be indicative of intermediate states during the folding/refolding pathway of a protein chain. In other words, it would appear that the folding of the mutant does not obey the classical two-state (native/denatured) pattern that the wild type displays. Interestingly, Kosinski-Collins and King[27] have shown that when hydrophobic pockets of wild-type human γD-crystallin are exposed (by adjusting the amount of Gdn HCl in the solution), the protein displays hysteresis and self-aggregation. Unfortunately, however, the solubility of the mutant γD-crystallin is remarkably low (<0.25 mg/mL, far lower than that of the wild type). Because of this, it has not been possible to explore the folding–refolding features of this molecule in greater detail using other experimental techniques at this low concentration. We have thus resorted to in silico comparison of the mutant and wild-type proteins using molecular modeling.

Structural Modeling of the Mutant Proteins

γD-Crystallin. Figure 3A shows the crystal structure of wild-type human γD-crystallin, retrieved from the protein database. The part of the structure shown in red (namely, the C-terminal fragment) is deleted in the mutant. The region of deletion includes the β strand between residues 166 and 170, and this β strand is a part of a β sheet, which is an integral component of the C-terminal domain. The region of deletion includes a few hydrophobic residues. Some of these hydrophobic residues, such as Val164 and Leu167, are completely buried in the wild type. Figures 3B and 3C show the interaction patterns in the hydrophobic pocket of the wild-type molecule

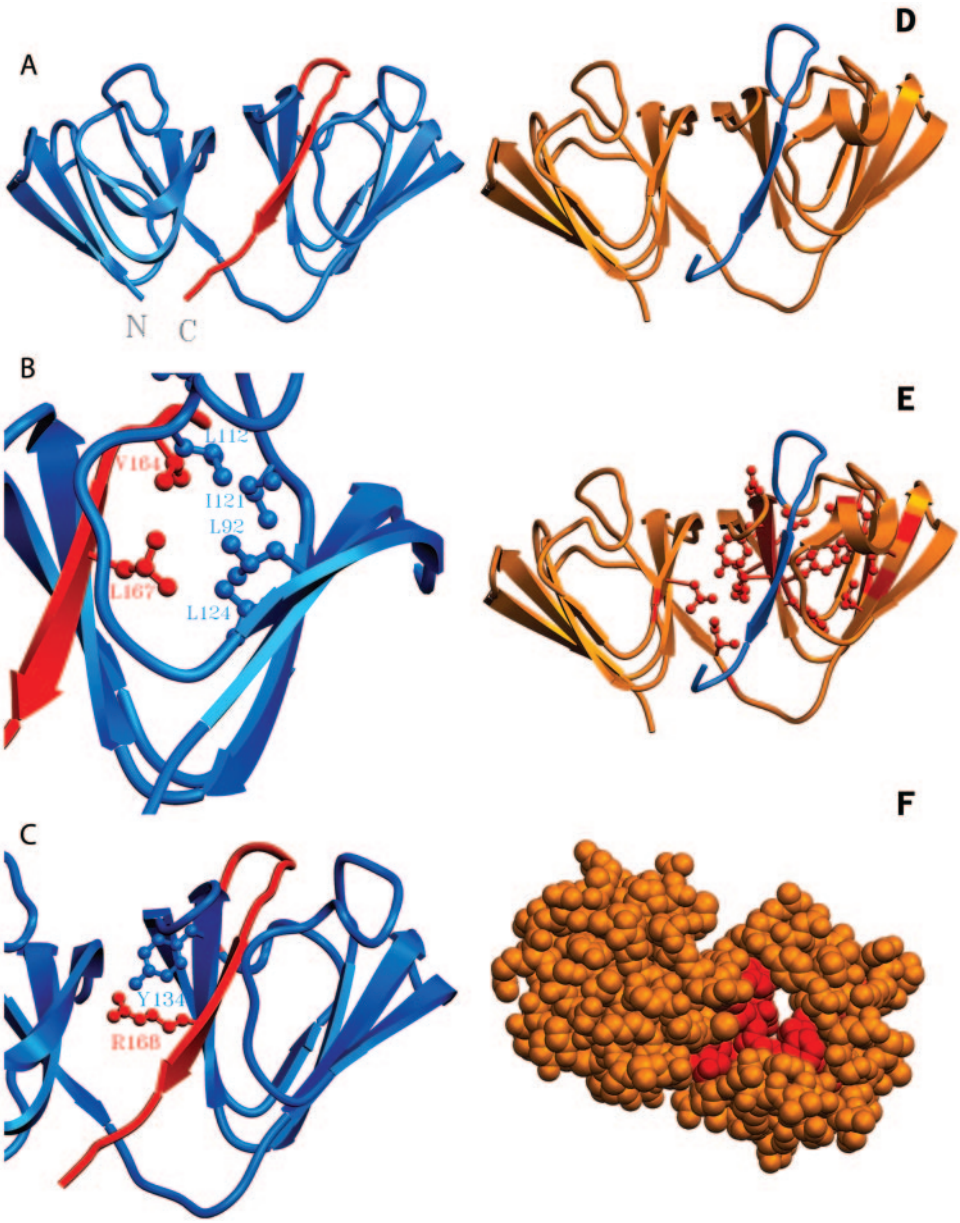

FIGURE 3. (**A**) Structure of human γD-crystallin retrieved from protein data bank. The part of the image shown in *red* is lost in the W156X mutant. (**B**) Model showing the hydrophobic pocket involving the amino acid residues from the deleted region and other parts of the protein. (**C**) Model showing the aromatic-cation interaction between Tyr134 and Arg168 located in the region of deletion. (**D**) Structure of wild-type human γC-crystallin. The part of the image shown in *red* is deleted in the mutant. (**E**) Interacting residues in the C-terminal region in the wild-type molecule, which are lost in the mutant. (**F**) Space-filling model of the mutant showing the continuous apolar patch.

(e.g., involving Leu112, Ileu121, Tyr134, Glu135, Val164, Leu167, and Arg168). The residues that undergo major solvent accessibility changes lose their interaction with their surroundings. Table 1 lists the residues, which are buried in the wild-type γD-crystallin but are exposed in the W156X mutant. The percentages were estimated with the help of the software GRASP, using the method described earlier.[11]

γC-Crystallin. Figure 3D shows the structure of the wild-type molecule, modeled on the basis of the crystal structure of bovine γB-crystallin, as described earlier.[11] Here again, the loss of the C-terminal 18 residues leads to notable effects in the tertiary and aggregational properties of the mutant, primarily caused by the exposure of several apolar residues (shown in Fig. 3E) buried by the C-terminal region in the wild type. A list of apolar residues buried (recognized by <7% solvent accessibility) in the wild type but exposed (>7% solvent accessibility) in the mutant is provided in Table 2. Figures 3D and 3E highlight this differential exposure, by which the mutant molecule is seen to present a continuous patch of hydrophobic side chains exposed to the surface. Figure 3F illustrates this continuous apolar patch.

Discussion

W156X is yet another example of mutation in human γD-crystallin associated with cataract; the others are R14C, P23T, R36S, and R58H. All these mutants display lower solubility in water than the wild-type molecule (<20 mg/mL for most of the mutants, <100 mg/mL for R14C, >200 mg/mL of the wild type; all at 20°C). The solubility of W156X is even lower (<0.25 mg/mL). The loss of the C-terminal 18 residues appears to have a more drastic effect on solubility. The C-terminal residues play a greater role in hydration, intermolecular interactions, and solubility. Crystal structural analysis of wild-type human γD-crystallin indicates the involvement of Asp156, Arg163, and Arg168 in charge interactions and of Phe173 in amine-aromatic interactions and hydrophobic interactions.[8] Not only are these lost in the deletion mutant, but, as Table 1 shows, several other residues in the rest of the sequence are now exposed to the solvent. Some of these are Leu112, which is in contact in the wild-type molecule with Val164 and Leu167; Ile121, which is in contact with Leu92, Leu124, and Val164; Val132, which interacts with Val170; the highly conserved, and thus crucial, Tyr134, which is well buried in the wild-type and is now exposed to a great degree in the mutant; and another conserved residue, the acidic Glu135, which had an ion pair interaction with Arg163 in the wild type is now left exposed.

All these changes affect not the secondary structure, or the chain conformation, of the molecule in any significant manner; much of the effect is in the tertiary structure and surface hydrophobicity of the molecule (Fig. 2). They lead, however, to a weakening of the stability of the mutant molecule, as seen by its easier denaturation.

It would thus seem that of all the mutants of human γD-crystallin, the consequence of the loss of the C-terminal 18 residues is more drastic, leading to significant loss of solubility and to self-aggregation and scattering particles. These are visualized in situ in cells.

Table 2 lists some of the apolar residues of the W157X mutant of human γC-crystallin that are buried by the C-terminal region in the wild-type molecule but are exposed in the mutant. Residues such as Leu57, Ile112, Ile121, Trp131, and Leu133, which are buried in the wild type, surface in the mutant. A few apolar residues, such as Leu105, are already exposed in the wild type and become even more so in the mutant. A few in the N-terminal domain and in the domain–domain interface of the structure have increased accessible surface area in the mutant because part of the deleted C-terminal region is involved in the interdomain interface. The overall increase in the solvent accessible surface area (ASA) in the mutant (compared with the wild type) is computed to be approximately 307 Å^2, of which 133 Å^2 are contributed by apolar side chains. Apart from this large increase in ASA, we observed a continuous hydrophobic patch in the mutant (Fig. 3F), which led to decreased aqueous solubility, self-aggregation, and scattering particles. These were again visualized when the cDNA of W157X human γC-crystallin was transfected into cells (Fig. 1).

The results presented in this article thus show that the loss of the C-terminal fragment in human γD- and in γC-crystallin leads to greatly reduced solubility of the molecule and to the formation of substantial intermolecular aggregates in a variety of cells, notably in human lens epithelial cells. Such aggregates would be expected to generate light-scattering particles, compromising the transparency of the cells and their assemblies.

Table 1. Residues Buried in the Wild-Type but Solvent Exposed in the W156X Mutant Human γD-Crystallin

No.	Residue	Accessibility in the Wild-Type γD-Crystallin (%)	Accessibility in the Mutant (%)
1	Leu112	0.0	14.9
2	Ile121	0.0	50.5
3	Val132	0.0	58.4
4	Tyr134	0.0	60.6
5	Glu135	0.0	64.0
6	Leu136	5.0	16.0

Table 2. Apolar Residues Buried in the Wild-Type but Solvent Exposed in the W157X Mutant of Human γC-Crystallin

Apolar Residue	Solvent Accessibility of the Side Chain in the Wild Type (%)	Solvent Accessibility of the Side Chain in the Mutant (%)
Leu57	0.7	24.8
Ile82	0.9	11.1
Leu90	1.8	8.1
Leu92	2.7	10.1
Ile112	3.7	31.9
Ile121	3.8	22.2
Leu124	0.1	8.1
Trp131	0.6	19.8
Val132	0.0	7.6
Leu133	0.2	39.1
Tyr134	3.3	16.3
Tyr144	3.5	43.4
Leu146	1.6	9.3
Tyr151	4.7	11.8

Acknowledgments

The authors thank Suraj Bhat for discussions.

References

1. Cartier M, Tsui L-C, Ball SP, Lubsen NH. Crystallin genes and cataract. In: Wright AF, Jay B, eds. *Molecular Genetics of Inherited Eye Disorders*. Newark, NJ: Harwood Academic Publishers; 1994: 413–443.

2. Bhat SP. Crystallins, genes and cataract. *Prog Drug Res*. 2003;60: 205–262.
3. Hejtmancik JF. The genetics of cataract: our vision becomes clearer. *Am J Hum Genet*. 1998;62:520–525.
4. Heon L, Priston M, Schorderet DF, et al. The gamma crystallins and human cataracts: a puzzle made clearer. *Am J Hum Genet*. 1999; 65:261–267.
5. Santhiya ST, Shyam Manohar M, Rawlley D, et al. Novel mutations in the γ-crystallin genes cause autosomal dominant congenital cataracts. *J Med Genet*. 2002;39:352–358.
6. Pande A, Pande J, Asherie N, et al. Molecular basis of a progressive juvenile-onset hereditary cataract. *Proc Natl Acad Sci U S A*. 2000;97:1993–1998.
7. Pande A, Pande J, Asherie N, et al. Crystal cataracts: human genetic cataract caused by protein crystallization. *Proc Natl Acad Sci U S A*. 2001;98:6116–6120.
8. Basak A, Bateman O, Slingsby C, et al. High-resolution X-ray crystal structures of human γD crystallin (1.25 A) and the R58H mutant (1.15 A) associated with aculeiform cataract. *J Mol Biol*. 2003;328: 1137–1147.
9. Evans P, Wyatt K, Wistow GJ, Bateman OA, Wallace BA, Slingsby C. The P23T cataract mutation causes loss of solubility of folded γD-crystallin. *J Mol Biol*. 2004;343:435–444.
10. Pande A, Annunziata O, Asherie A, Ogun O, Benedek GB, Pande J. Decrease in protein solubility and cataract formation caused by the Pro23 to Thr mutation in human gamma D-crystallin. *Biochemistry*. 2005;44:2491–2500.
11. Talla V, Narayanan C, Srinivasan N, Balasubramanian D. Mutation causing self-aggregation in human γC-crystallin leading to congenital cataract. *Invest Ophthalmol Vis Sci*. 2006;47:5212–5217.
12. Fu L, Liang JJ. Conformational change and destabilization of cataract γC-crystallin T5P mutant. *FEBS Lett*. 2002;513:213–216.
13. Kmoch S, Brynda J, Asfaw B, et al. Link between a novel human γD-crystallin allele and a unique cataract phenotype explained by protein crystallography. *Hum Mol Genet*. 2000;9:1779–1786.
14. Prasher DC, Eckenvode VK, Ward WW, Prendergast FG, Cormier MJ. Primary structure of the *Aequorea victoria* green-fluorescent protein. *Gene*. 1992;111:229–233.
15. Chalfie M, Tu Y, Euskirchen G, Ward WW, Prasher DC. Green fluorescent protein as a marker for gene expression. *Science*. 1994;263:802–805.
16. Inouye S, Tsuji FI. Evidence for redox forms of the *Aequorea* green fluorescent protein. *FEBS Lett*. 1994;341:277–280.
17. Sun TX, Das BK, Liang JJ. Conformational and functional differences between recombinant human lens αA- and αB-crystallin. *J Biol Chem*. 1997;272:6220–6225.
18. Lindley PF, Najmuddin S, Bateman O, et al. Structure of the bovine gamma-B crystallin at 150K. *J Chem Soc Faraday Trans*. 1993;89: 2677.
19. Sali A, Blundell TL. Comparative protein modeling by satisfaction of spatial constraints. *J Mol Biol*. 1993;339:1103–1113.
20. Evans SV. SETOR: hardware lighted three-dimensional solid model representations of macromolecules. *J Mol Graphics*. 1993;11:134–138.
21. Wang K, Cheng C, Li L, et al. γD-crystallin-associated protein aggregation and lens fiber cell denucleation. *Invest Ophthalmol Vis Sci*. 2007;48:3719–3728.
22. Pigaga V, Quinlan RA. Lenticular chaperones suppress the aggregation of the cataract-causing mutant T5P γC-crystallin. *Exp Cell Res*. 2006;312:51–62.
23. Sinha D, Esumi N, Jaworski C, Kozak CA, Pierce E, Wistow G. Cloning and mapping of the mouse Crygc gene and non-lens expression of γS-crystallin. *Mol Vis*. 1998;4:8.
24. Zhang C, Gehlbach P, Gongora C, et al. A potential role for β- and γ-crystallins in the vascular remodeling of the eye. *Dev Dyn*. 2005;234:36–47.
25. Mandal K, Kono M, Bose SK, Thomson J, Chakrabarti B. Structure and stability of gamma-crystallins, IV: aggregation and structural destabilization in photosensitized reactions. *Photochem Photobiol*. 1998;47:583–591.
26. Cardamone M, Puri NK. Spectrofluorimetric assessment of the surface hydrophobicity of proteins. *Biochem J*. 1992;282:589–593.
27. Kosinski-Collins MS, King J. In vitro unfolding, refolding, and polymerization of human γD crystallin, a protein involved in cataract formation. *Protein Sci*. 2003;12:480–490.